Science of the Total Environment 929 (2024) 172677

Contents lists available at ScienceDirect

Science of the Total Environment

journal homepage: www.elsevier.com/locate/scitotenv

Recovery of cellulose acetate bioplastic from cigarette butts: realization of a sustainable sorbent for water remediation

Massimo Giuseppe De Cesaris [a], Nina Felli [a], Lorenzo Antonelli [a], Iolanda Francolini [a], Giovanni D'Orazio [b], Chiara Dal Bosco [a], Alessandra Gentili [a,*]

[a] Department of Chemistry, Sapienza University, P.le Aldo Moro 5, 00185 Rome, Italy
[b] Istituto per i Sistemi Biologici (ISB), CNR - Consiglio Nazionale delle Ricerche, Montelibretti, Rome, Italy

HIGHLIGHTS

- Cigarette filters are one of the most abundant and hazardous wastes in the world.
- A simple strategy to recover cellulose acetate (CA) from this harmful waste is proposed.
- A porous composite CA-based cryogel was prepared in combination with carbon powder.
- The composite 3D-membranes were tested for water remediation.
- Organic contaminants, selected as model compounds, were efficiently and quickly removed.

GRAPHICAL ABSTRACT

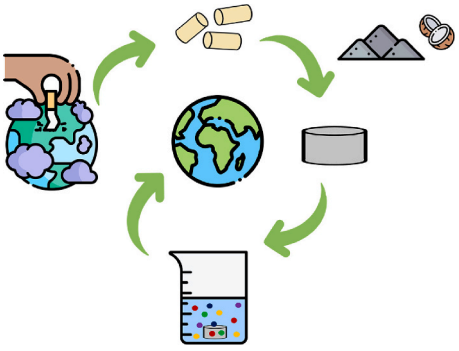

ARTICLE INFO

Editor: Damia Barcelo

Keywords:
Bioplastic
Recycled cellulose acetate
Composite sorbents
Organic contaminants
Water treatment
Sustainable chemistry

ABSTRACT

Cigarette butts, one of the most common forms of litter in the world, represent a source of chemical and plastic pollution releasing thousands of toxic compounds and microfibers of cellulose acetate (CA). Besides the correct waste management, the recovery of CA from cigarette filters is a way to cushion their negative effects on the environment. Thus far, recycling strategies have been limited to industrial applications, while not many solutions have designed for water remediation. This work describes a strategy to valorize this harmful waste and to reverse its environmental impact, proposing a simple and effective procedure of reclamation of CA and its reuse to prepare a composite sorbent for the treatment of polluted water. The first step entails the washing of filters with hot water (T = 90 °C) and hot ethanol (T = 58–68 °C) to remove the impurities produced during cigarette burning, as verified by means of UV and attenuated total reflection-Fourier-transform infrared (ATR-FTIR) spectroscopy, thermal gravimetric analysis (TGA), and differential scanning calorimetry (DSC). The second step involves the use of the regenerated CA to prepare porous cylinder-shaped cryogels (15 mm × 10 mm) whose sorption properties are enhanced by the combination with AC (15 % w/w). The synthesis takes advantage of the sol-gel transition of the polymer dispersion (5 % w/V) in a solution acetone/water 5 mM in NH_3 (60/40, v/v). After characterization by dynamic mechanical analysis (DMA), TGA, FT-IR, and scanning electron microscopy (SEM), the adsorption capability of the physical cryogel was studied in terms of treated environmental water volume, contact time and concentration of the selected pollutants. The results have shown that the proposed

* Corresponding author.
E-mail address: alessandra.gentili@uniroma1.it (A. Gentili).

https://doi.org/10.1016/j.scitotenv.2024.172677
Received 20 February 2024; Received in revised form 19 April 2024; Accepted 20 April 2024
Available online 24 April 2024

strategy is a low-cost way to recycle CA from cigarette butts and that the designed sorbent is a promising material for water treatment, allowing quick removal times and yields >79.6 %.

1. Introduction

Only in 2022, six trillion cigarettes were smoked worldwide producing 500 million kilograms of waste (Bonanomi et al., 2015). Each year these figures increase and, besides the reasons related to the smokers' health, they are worrying because >70 % of burnt butts are littered into the environment (Shah et al., 2023), leaching nicotine, heavy metals, polycyclic aromatic hydrocarbons, phthalates (Vasseghian et al., 2023), pesticides (D'Ascenzo et al., 1998), and thousands of other compounds (Novotny and Slaughter, 2014). Studies on the dynamics of these pollutants have highlighted how they can be released once filters are subjected to atmospheric agents, ending up contaminating various environmental compartments (Moroz et al., 2021). The toxicity of these pollutants is manifested by both acute and chronic effects on numerous aquatic and terrestrial organisms (fish, insects, small mammals, amphibians, etc.) and plants, even at relatively low doses (Moroz et al., 2021). The spread of cigarettes is also associated with the emerging issue of microplastic pollution (Marinello et al., 2020). In fact, 97 % of cigarette filters (CFs) are made of microfiber bundles of cellulose acetate (CA) (Puls et al., 2011), a polymer which is categorized as a 'bioplastic' since it is obtained by esterification of cellulose with acetic acid. Depending on the environmental conditions, cigarette butts (CBs) can take up from 5 to 14 years to entirely dissipate because of their resistance to fungal and bacterial degradation imparted by acetylation (Green et al., 2022). In 2017, World Health Organization published a report illustrating the quieter but shockingly widespread impacts of tobacco from an environmental perspective, explaining how CBs are one of the most polluting forms of littering (Bialous et al., 2017). In Italy, the 2015 Green Economy law (Legge 28.12.2015, n. 221) provides for a fine (from a minimum of 60 euros to a maximum of 300 euros) for those who throw small waste, including CBs, chewing gums and receipts, on the ground. Given the poor results of these punitive measures regulating citizen's behaviors, Italy as well as other Member States of the European Union decided to adopt the Extended Producer Responsibility (EPR) scheme (Kosior and Crescenzi, 2020) to make manufacturing companies responsible for the management and disposal of products placed on the market. As required by the European Single Use Plastic (SUP) Directive of 2021 (Directive UE 2019/904, 2019), the EPR for waste tobacco products came into force on 5 January 2023. The EPR concerns two aspects in particular: the management of waste from tobacco products to contain littering, and awareness campaigns aiming at informing consumers. In 2022, four big players on the Italian market supported the Erion Care consortium (ErionCare, https://erioncare.it/it/) to define a national program agreement with municipalities and urban hygiene service managers; the major objectives of the consortium are the development of collection points and the promotion of the pocket ashtray distribution. Currently, since there has not been specific separate collection yet, CBs are dropped off into unsorted waste containers ending up in landfill or waste-to-energy plants. Thus, while the problem of the collection phase is being addressed, it is important to seek solutions for recycling this problematic waste.

In the virtuous vein of "cleaning the environment by recycling waste", the literature reports several examples of CB recycling: from the infrastructure sector, used as fillers and binders to make bricks, road paving or insulation materials, to the energy, metallurgical, cosmetic and medical sectors (Conradi and Sánchez-Moyano, 2022). CBs are also recycled to make nanomaterials in the paper industry (Marinello et al., 2020), and environmental engineering for the removal of organic contaminants (Torkashvand and Farzadkia, 2019), oils (Nabwey et al., 2024), dyes (Fahanwi et al., 2024), drugs (Antonelli et al., 2024), and heavy metals (Torkashvand et al., 2022) from aqueous matrices (Moroz et al., 2021). Regarding these last applications, some papers deal with the fabrication of active carbon from CFs for the adsorption of methylene blue, after alkaline activation combined with microwave heating (Hamzah and Umar, 2017) or low-temperature hydrothermal carbonization (Lima et al., 2018). However, not many papers cope with the recovery of the raw polymer from CFs of smoked cigarettes to prepare sorbent materials (Mahto et al., 2022; Abu-Danso et al., 2019). In the work by Mahto et al. (2022), the recycling process of CA involves a washing step followed by dissolution, filtration, and reprecipitation to prepare flat-sheet semi-permeable membranes to be used for the removal of dyes and monovalent and divalent salts from water samples. Instead in the work by Fahanwi et al. (2024), CFs were processed to produce electrospun CA nanofibrous membranes modified with polyaniline for the adsorption of anionic and cationic dyes (methyl orange and rhodamine chloride) from an aqueous phase with removal yields of 99 % and 55 %, respectively. Abu-Danso et al. (2019) treated CA nanofibers with 5 % (w/v) NaOH solution for 6 h at 60 °C to obtain cellulose, which was then etched with phosphate ions; the functionalized cellulose nanofibers could retain diclofenac from water samples with a maximum removal capacity of 107.90 mg/g. However, most of the applications of the literature are related to the direct use of the regenerated polymer (CA or cellulose) for the removal of a few inorganic (metal ions) or organic polar contaminants such as dyes. On the other hand, the combination of CA with other (nano)materials could extend the applicability to low polar organic contaminants including many harmful chemicals, such as pesticides, drugs, hormones, personal care products, etc. Since CA is particularly suitable to prepare composite semi-permeable gels (Wang and You, 2021), the wide variety of sorbents that can be obtained can justify the recovery of CBs and their introduction within cyclic production realities.

Within the described context, the present work puts forward a simple, fast, and low-cost procedure to recover CA from CBs, and to prepare a sustainable composite sorbent for water remediation purposes. To this end and to the best of our knowledge, for the first time the CA recovered by CBs was used for the synthesis of porous cryogels in which activated carbon (AC) from agri-food waste was dispersed. All cryogels had the shape of a 3D membrane and were morphologically and structurally characterized by thermal, mechanical, and spectral analyses. The membranes with different loads of AC were then used to evaluate their capability of purifying river water samples from eleven common organic contaminants belonging to several chemical classes. The maximum amount of water treated, the concentration of the pollutants, and the adsorption kinetics were also studied. The principal aim of this study is to propose a strategy to valorize this harmful waste, source of chemical and plastic pollution, and to reverse its environmental impact by regenerating and transforming the plastic component of CFs to mitigate the presence of organic contaminants in environmental waters.

2. Materials and methods

2.1. Chemicals

Diclofenac, ibuprofen, ketoprofen, sulfadiazine, sulfaguanidine, carbaryl, chlorsulfuron, cinosulfuron, linuron, and atrazine were purchased from Aldrich–Fluka–Sigma S.r.l. (Milan, Italy). Fenthion was bought from Dr. S. Ehrenstorfer Promochem (Wesel, Germany). All standards had a purity grade >93 %.

Ethanol (96 %), acetone (>99.8 %), ammonia (28–30 %), formic acid (98 %), methanol (>99.8 %), and acetonitrile (>99.8 %) were purchased from Aldrich–Fluka–Sigma S.r.l. (Milan, Italy). Ultrapure water was obtained from a Milli-Q water generator (Millipore, Bedford, MA,

USA). Edible AC, produced by pyrolysis of coconut shells, was purchased from Special Ingredient Europe.

The individual stock solutions of each analyte were prepared dissolving weighed standard amounts (OHAUS DV215CD Discovery Semi-Micro and Analytical Balance 81 g/210 g capacity, 0.01 mg/0.1 mg readability) in methanol at a concentration of 1 g/L. A composite working solution was prepared by diluting the individual stock solutions in methanol at a concentration of 100 μg/L. All the solutions were stored at 4 °C.

2.2. Water samples

All investigation was performed using river water samples gathered from Tiber River in the Farfa Oasis (a natural reserve near Rome). The sampling was performed following the "Regional Agency for the protection of the environment" (Agenzia Regionale per la Protezione Ambientale, ARPA) guidelines, which provide methodologies and procedures for a representative sampling. Briefly, five 1-L samples were collected in amber glass bottles and transported to the laboratory under cooled conditions (4 °C). Upon reception, samples were filtered through 0.45 μm Nylon filters (Whatman, Maidstone, UK) to eliminate particulate matter and other suspended solids and then stored at 4 °C in the dark. A preliminary analysis of the samples did not detect the presence of any contaminants at concentrations higher than the LOD of the method (Sections 2.10 and 3.3).

2.3. Cigarette butts and filters

Pristine filters from different commercial brands were used as reference materials to verify the efficiency of the developed cleaning protocol of filters from CBs.

CBs, from different commercial brands, were collected in a disposal container located in Sapienza University of Rome. CFs were obtained by removing wrapping paper, unburned tobacco, and ashes from the collected butts.

2.4. Recovery of cellulose acetate from cigarette filters

Dirty CA filters were cut along the longitudinal axe to open and stretch the fibers stiffened by heat. Then, the fibers were washed with hot water (T = 90–100 °C) for 15 min and, finally, with ethanol 96 % (T = 58–68 °C) for other 15 min under gentle stirring. Approximately, 200 mL of each solvent was required for every 1.5 g of CFs. Finally, the clean filters were dried in an oven at T = 30 °C for 1 h. Ethanol was recycled by distillation. Fig. S1 in the Supplementary Material shows the main steps of the washing protocol.

2.5. Synthesis of cryogels

The 5 % w/v colloidal solution of CA was prepared by dispersing the regenerated polymer fibers in acetone/water containing 5 mM NH_3 (60:40, v/v). The solution was allowed to rest for 30 min to ensure the solvent penetration into fibers; afterward, it was stirred for 2 h at room temperature until a homogenous solution was obtained. A 4-mL volume was transferred into a cylindrical plastic mold (diameter = 15 mm) and left to rest overnight to guarantee the sol/gel transition of the colloidal solution. Then, the obtained organogel was immersed in Milli-Q water for 8 h to switch the polymer dispersant phase from the organic to the aqueous phase. Lastly, the hydrogel was frozen at −20 °C overnight and freeze-dried for 12 h to obtain a cylinder-shaped cryogel (Fig. S2).

The composite cryogel was prepared following the same procedure with some modifications. After dissolving and stirring the polymer, AC powder (15 w/w referred to the polymer weight) was added to the colloidal solution. The solution was stirred for 20 min, sonicated for other 20 min to ensure the homogeneous dispersion of the carbon powder, and finally molded, frozen, and lyophilized to obtain a composite cryogel with a cylindrical shape (CA@AC-15 %). Other cryogels containing 5 % (CA@AC-5 %), and 10 % (CA@AC-10 %) of AC were also prepared according to the same procedure. Finally, to obtain rotating devices, each cryogel was trapped into a polypropylene mesh pouch, provided with a side pocket to host a magnetic stir bar.

2.6. Characterization of the recovered cellulose acetate

The effectiveness of the filter cleaning protocol, described in Section 2.4, was evaluated by comparing recovered CA with the pristine one from unused CFs.

UV–Vis spectra were collected (T60 UV–Vis spectrophotometer, PG instrument Ltd.) in the range 190–450 nm by analyzing 0.5 % w/v CA solutions obtained dissolving 50 mg of pristine filters, recovered filters and dirty filters (unwashed) in 10 mL of acetone. Afterward, the polymer was precipitated by casting the solvent and characterized by attenuated total reflection-infrared spectroscopy (ATR-FTIR), thermogravimetric analysis (TGA), and differential scanning calorimetry (DSC).

The ATR-FTIR spectra were recorded in the spectral range between 650 and 4000 cm^{-1} at a resolution of 2 cm^{-1} and co-adding 100 scans by using a spectrophotometer Nicolet 6700 (Thermo Fisher Scientific, Waltham, MA, USA), equipped with a Golden Gate single reflection diamond ATR accessory.

The thermogravimetric analyses were performed with a thermobalance Mettler TG 50 (Mettler Toledo, Columbus, OH, USA) by using a temperature ramp, from 25 to 650 °C, with a heating rate of 10 °C/min under N_2 flow.

The DCS analyses were carried out with a DSC Mettler Toledo DSC 822e (Mettler Toledo, Greifensee, Switzerland) by setting a temperature ramp with a heating rate of 10 °C/min under N_2 flow in the temperature range 25–300 °C.

2.7. Characterization of the synthesized cryogels

The synthesized cryogels (without AC and CA@AC-15 %) were characterized by means of TGA, ATR-FTIR, DMA, and SEM. The gravimetric method was used to determine the total porosity of the cryogels, while a liquid displacement method was applied to obtain information on pore interconnectivity (Wienk et al., 1994).

The same TGA and ATR-FTIR instrumental configurations, described in Section 2.6, were used to characterize all the cryogels.

The mechanical properties of the cylinder-shaped cryogels (15-mm diameter and 10-mm height) were studied by compression tests. To this end, a Force Measurement Imada instrument (Imada Co., Ltd.) applied a constant deformation rate of 10 mm/min, with an average applied strength of 17 N; the maximum piston displacement distance was set at 4.5 mm, corresponding to approximately half the height of the device. The compression modulus was determined by the slope of the linear section of the stress-strain curve in a range of deformation lower than 10 %.

The determination of the total cryogel porosity (*P%*) required the preliminary measurement of the apparent density, $\rho_c = \frac{m}{V}$, where m and V were the weight and the volume of the examined cryogels, respectively. *P%* was calculated as follows:

$$P\% = \left(1 - \frac{\rho_C}{\rho_p}\right) * 100 \quad (1)$$

The polymer density, ρ_p, was evaluated as an intermediate value between the average density of CA (ρ_{CA} = 1.3 g/cm^3) and the average density of cellulose (ρ_C = 1.5 g/cm^3) due to the deacetylation reaction of CA that occurs during the synthesis of the cryogels.

A liquid displacement method was used to obtain information on open pore interconnectivity (*OP%*). A cryogel, with weight W_0 (90–150 mg) and volume V_0 (1.65–1.85 cm^3), was dipped in a volume V_{EtOH} of ethanol (10 mL) for 30 min. Ethanol (density 0.806 g/cm^3 at 20 °C) was

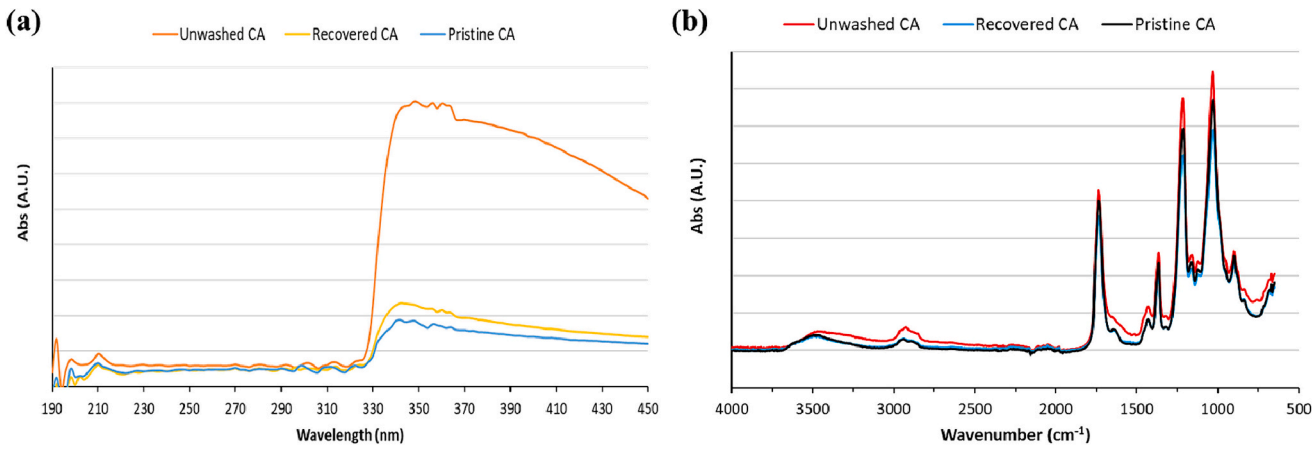

Fig. 1. **(a)** UV adsorption band of 0.5 % w/v CA solutions in acetone, obtained using unwashed CA, recovered CA and pristine CA. **(b)** ATR-FTIR spectra of unwashed CA, recovered CA, and pristine CA; the efficacy of the cleaning protocol is highlighted by the overlapping of pristine and recovered CA spectra and from the characteristic CA adsorption band.

chosen because it is a non-solvent for the polymer and does not cause swelling phenomena. Therefore, the scaffold was removed and weighted (W_1). Finally, *OP%* was determined by the following equation:

$$OP\% = \left(\frac{W_1 - W_0}{\rho_{EtOH} * V_{EtOH}}\right) * 100 \quad (2)$$

The morphological structure of the cryogels was studied by means of SEM (LEO 1450 VP, Carl Zeiss, Oberkochen, Germany). Before the scanning process, all samples were dried and coated with chromium to make their surface conductive. The micrographs obtained were taken at different magnifications (100–500 X), using 14 mm as working distance, 15 kV as accelerating voltage, and DISS as digital image recording.

2.8. Ultra-high-performance liquid chromatography-tandem mass spectrometry (UHPLC-MS/MS)

Liquid chromatography was performed by using a UHPLC-MS/MS system (ACQUITY HPLC H-Class PLUS system, Waters Corporation, Milford, MA, USA) provided with a quaternary pump, high-pressure mixing system, a column oven, and an autosampler. The eleven analytes were separated on an XTerra C18 column (250 × 4.6 mm, 3.5 μm) equipped with a pre-column of the same type. The mobile phase was water (phase A) and acetonitrile (phase B), both 2 mM in formic acid. The analyte separation was conducted at a flow rate of 1 mL/min maintaining 60 % of phase A for 10 min and then, reducing to 0 % until the end of the run (run time = 30 min); the injection volume was 40 μL.

The analytes were detected and quantified by an API 4000 Qtrap mass spectrometer (ABSCIEX, Foster City, CA, USA) whose Turbo V source was equipped with an electrospray ionization (ESI) probe. The detection was performed in dual polarity by setting the capillary voltage at 5500 V for the positive ionization and at −4500 V for the negative one. The source heater temperature was set at 450 °C to warm the drying gas. High-purity nitrogen was used as curtain gas (5 L/min) and collision gas (4 mTorr), while air was used as nebulizer gas (2 L/min) and drying gas (20 L/min). Unit mass resolution (0.7 ± 0.1 *m/z* full width at half-maximum, FWHM) was set in each mass-resolving quadrupole. The quantitative analysis of the target analytes was carried out in multiple reaction monitoring (MRM) mode, selecting two MRM transitions per analyte. Table S1 lists the UHPLC-ESI(±)-MRM parameters employed for identification and quantification purposes. Fig. S3 shows the chromatogram of a working standard solution. UHPLC-MS/MS data were acquired and elaborated by Analyst *v* 1.6 software (AB Sciex).

2.9. Adsorption tests and kinetics study

Batch adsorption tests were performed to evaluate the capability of the material to capture contaminants with different logP and pKa values from aqueous solutions. For this, CA@AC cryogels (5, 10, 15 % of AC) were immersed into different volumes (20 mL, 100 mL) of river water samples spiked at different concentrations (5 μg/L, 50 μg/L, 100 μg/L). Each test was carried out stirring at 200 rpm and room temperature. The optimal contact time was studied in the temporal range of 1–24 h and the analyte concentration was determined by injecting 100 μL of the water sample directly into the UHPLC-MS system, until the contaminant concentration either was not detected anymore or reached an equilibrium.

The performance of the removal process (%R) was calculated as the percentage of sorbate (contaminant) removed from the solution by the sorbent using the following mathematical expression (1):

$$\%R = \frac{C_0 - C_t}{C_0} \; x \; 100 \quad (3)$$

where C_0 is the original analyte concentration (μg/L) and C_t is the analyte concentration at a given time t (μg/L). Presuming that all the removed contaminant remains in the sorbent, one can estimate the concentration of the analyte in the material at time t, qt (mg/g) using:

$$q_t = \frac{(C_0 - C_t)}{m} \; x \; V \quad (4)$$

where V (L) is the volume of the solution and m (g) the mass of sorbent. When the equilibrium is reached, the eq. (4) can be rewritten taking into account that $t = t_e$, $q_t = q_e$ and $C_t = C_e$. The maximum adsorption capacity of the composite sorbent (q_e) was calculated based on $q_e = \frac{C_0 - C_e}{m} x \; V$.

For the kinetic studies, non-linear pseudo-first order (5) and pseudo-second order (6) models were evaluated to elucidate the mechanism involved in the adsorption process:

$$q_t = q_e\left(1 - e^{-k_1 t}\right) \quad (5)$$

$$q_t = \frac{k_2 q_e^2 t}{1 + k_2 q_e t} \quad (6)$$

where k_1 (min^{-1}) and k_2 (g/(g min)) are the pseudo first order and pseudo second order adsorption rate constants, respectively, and q_t is the amount of contaminant adsorbed (mg/g) at time t (min).

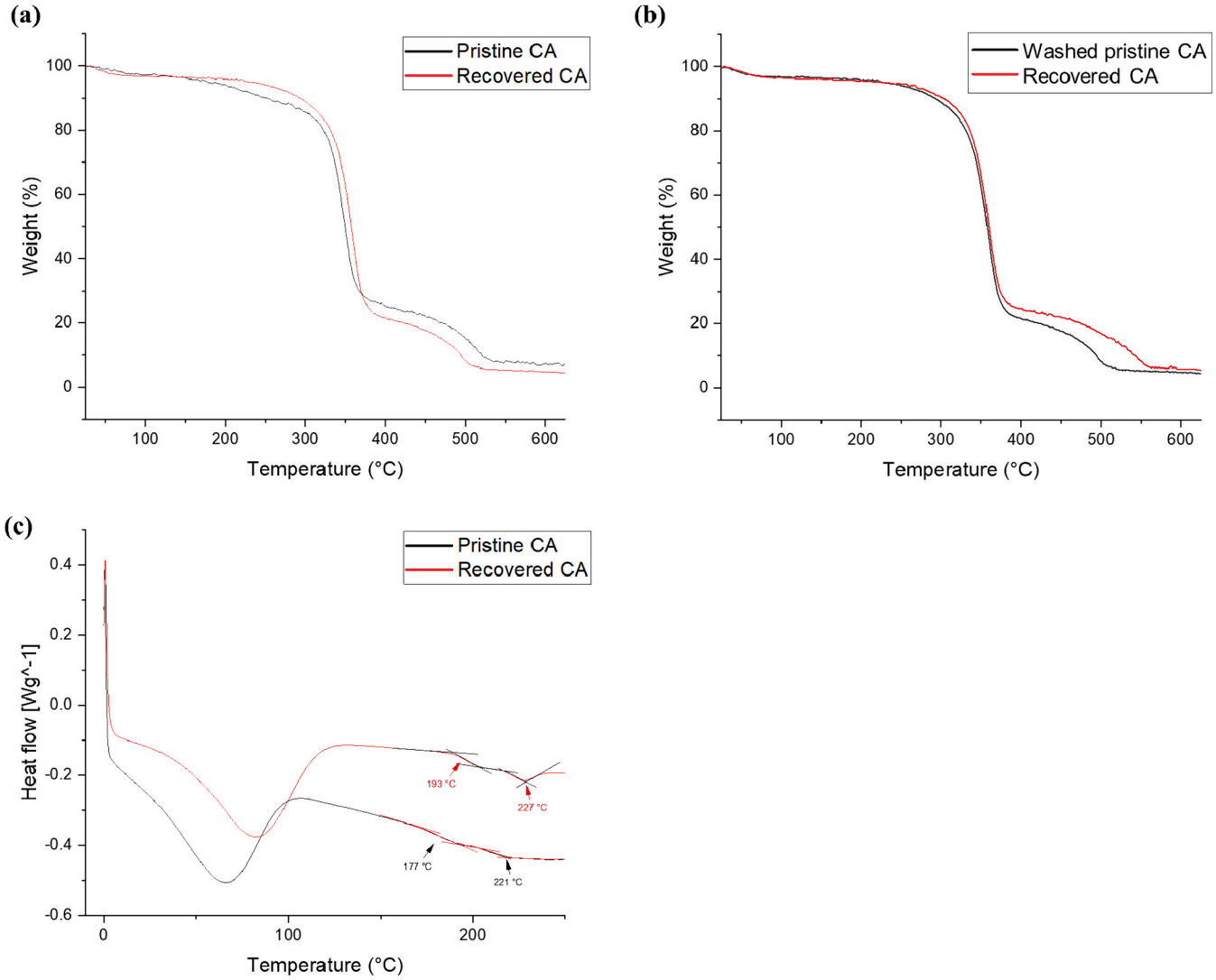

Fig. 2. Comparison of the TGA thermograms of recovered CA with pristine CA **(a)** and washed pristine CA **(b)**. **(c)** DSC curves of pristine and recovered CA.

2.10. Method validation

For the adsorption and kinetics studies, 100 μL of the water sample was directly injected into the UHPLC-MS/MS system. The analytes were quantified using the external calibration method. The calibration curves were built by spiking eleven 20-mL river water samples (Section 2.2) with increasing concentrations of the analytes (0.1, 0.25, 0.5, 1, 2.5, 5, 10, 25, 50, 75, 100 μg/L).

For each analyte, LOD was calculated as the spike level of a real water sample capable of providing a signal three times more intense than the noise (S = 3 N). The limit of quantification (LOQ) was estimated similarly but considering S = 10 N. Five replicates were carried out for the calculation of both LOD and LOQ. Precision was evaluated by analyzing five water samples spiked the analytes at 0.5 and 50 μg/L.

3. Results and discussion

3.1. Recovery of cellulose acetate

About 90 % of cigarettes are made up of CA fibers, compressed and kept together by glues and wrapping papers (Hamzah and Umar, 2017). The CA present in CFs is produced through two steps involving an initial acetylation of cellulose to obtain cellulose triacetate, followed by its partial hydrolysis to reduce the average degree of substitution to 2–2.5 per glucose unit, making CA (diacetate) more easily processable (Hummel, 2004).

In this work, a fast, simple, and cheap washing protocol was studied to remove substances adsorbed on CFs during combustion. The systematic comparison of the recovered CA with the pristine polymer from unused CFs was performed by using different instrumental techniques (UV spectroscopy, TGA, DSC, and ATR-FTIR) to select the more suitable procedure. Fig. S4 shows the aspect of CA fibers before and after washing.

3.1.1. UV–Vis spectroscopy

CA solutions (0.5 % w/v in acetone) from pristine, clean, and unwashed CFs were analyzed in the spectral range between 190 and 450 nm (see Section 2.6). Fig. 1a shows a characteristic band (330–350 nm) common to all three materials but different in intensity. The spectra profiles of reference CA and recovered clean CA appear very similar, while a strong absorption was observed for unwashed CA. This latter solution exhibited a yellow-orange coloration, probably due to the presence of conjugated compounds like polyaromatic hydrocarbons and aromatic amines that are generated during the burning of cigarettes (Soleimani et al., 2022). In this same spectral range, the absorption observed for pristine CA can be related to some additives, as also confirmed by the results of thermal analysis (see Section 3.1.3) (De Fenzo et al., 2020).

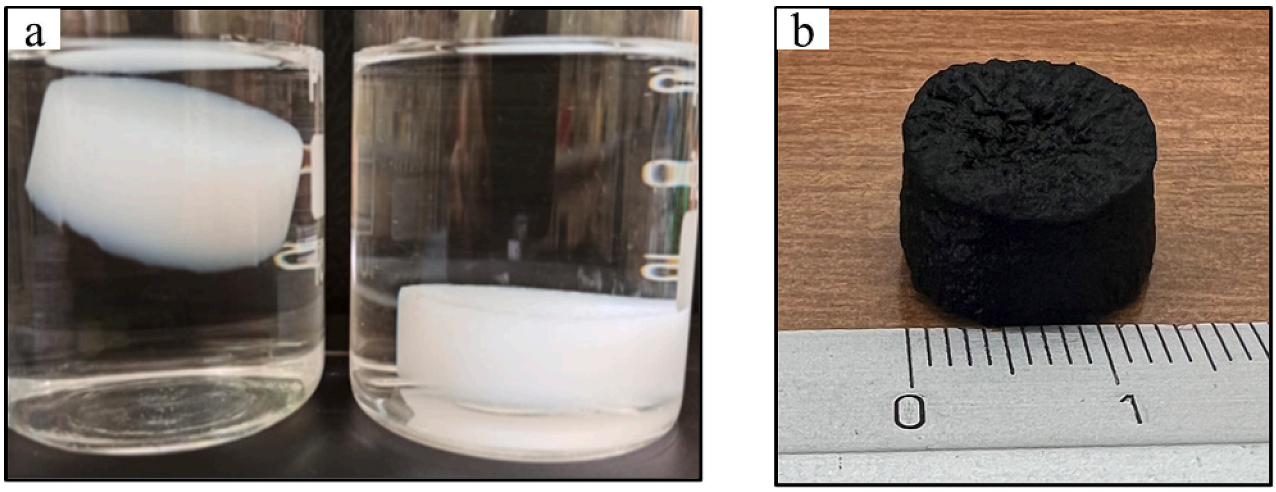

Fig. 3. **(a)** Gels obtained from the gelling process of CA solutions in the studied conditions. **(b)** The composite cryogel CA@AC-15 %.

The reduction in the absorption band of clean CA and its tendency to overlap to the pristine CA signal suggests an efficient removal of most impurities already after 30 min of washing. Different cleaning times (30, 40, 50, and 60 min) were tested but no evident difference was observed increasing the contact time.

3.1.2. ATR-FTIR spectroscopy

The recovered clean CA was investigated using ATR-FTIR spectroscopy in a spectral range between 400 and 4000 cm^{-1} and compared with pristine and unwashed CA (Fig. 1b). In all cases the characteristic bands of CA are observed. The broad absorptions between 3500 and 3000 cm^{-1} and 3000–2750 cm^{-1} are due to the O—H stretching of the hydroxyl groups and to the C—H stretching of the methyl groups of glucose, respectively. The band between 1750 and 1730 cm^{-1} is due to the C═O stretching of the ester bond, while the C—O stretching of the ester bond and secondary alcohols are observed in the range 1210–1163 cm^{-1} and 1120–1090 cm^{-1}, respectively. The O—H bending was observed between 1420 and 1330 cm^{-1} and that of C—H bending at wavenumber values <800 cm^{-1}.

The spectrum of unwashed CA shows the absorption bands associated with CA, along with some variations, particularly in the spectral range of 1700–1500 cm^{-1}. These differences are presumably related to the absorption of functional groups belonging to substances generated during the burning process. After washings, the overlap of the spectra of the pristine and regenerated CA suggests an efficient cleaning of the recovered polymer.

3.1.3. Thermal analysis (TGA, DSC)

The thermal properties of pristine CA and recovered CA were investigated by means of TGA and DSC analyses. Fig. 2a shows their TGA decomposition curves. For both polymers, a 3 % weight loss is observed between 27 and 127 °C due to the sample dehydration. For pristine CA, the following 10 % loss in the temperature range 127–338 °C is probably due to the loss of a plasticizer, added to facilitate the processing of CA

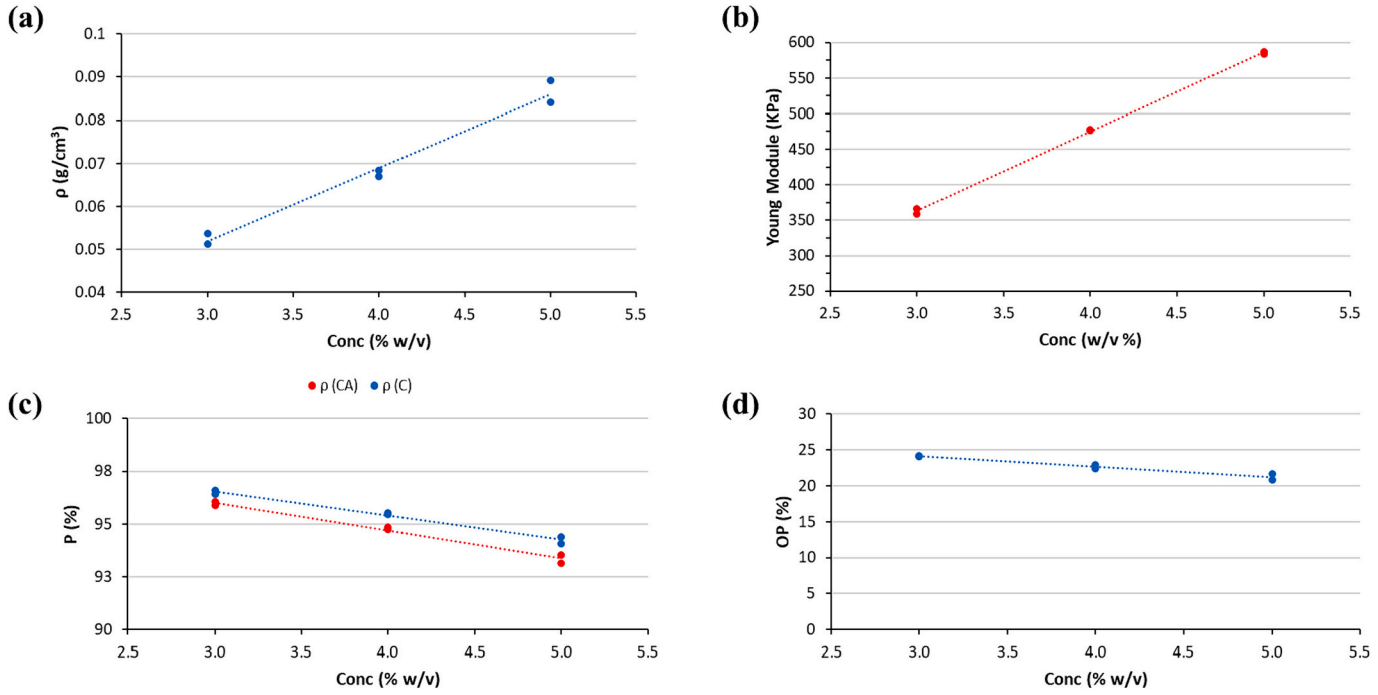

Fig. 4. **(a)** Variation of the cryogel density as a function of polymer concentration in solution. **(b)** Young module of cryogels; the plot shows how more deformation-resistant materials are obtained by increasing polymer concentration. **(c)** Total porosity and **(d)** open porosity of the synthesized material.

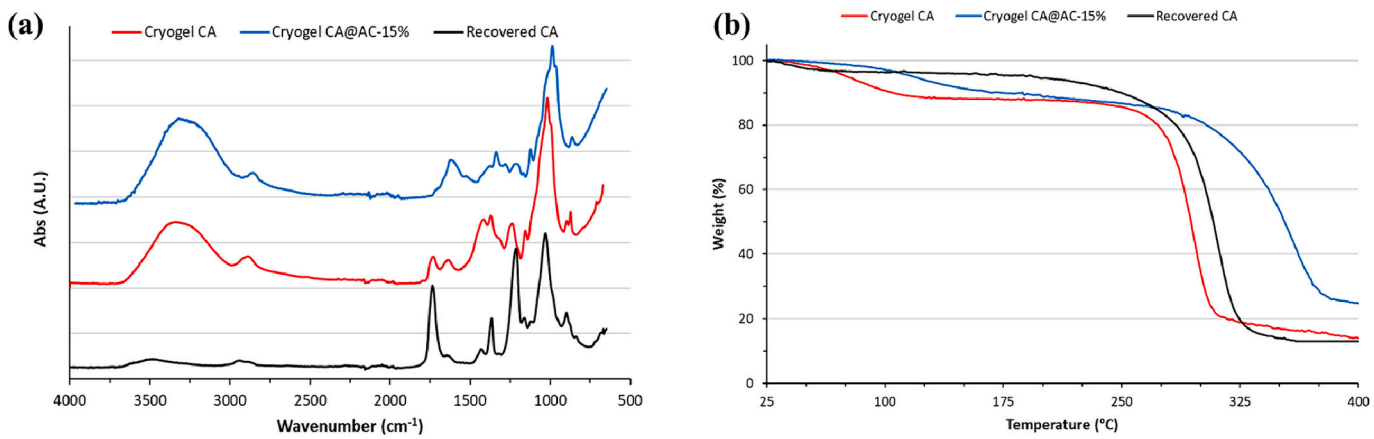

Fig. 5. Comparison among recovered CA and synthesized cryogels (CA and CA@AC-15 %) relying on characteristic ART-FTIR absorption bands **(a)** and thermal degradation curves **(b)**.

fibers (De Fenzo et al., 2020); such a process was not observed for recovered CA because the plasticizer was supposed to be removed during the filter cleaning. This hypothesis was confirmed by submitting the pristine CA to the same washing protocol and observing the disappearance of the weight loss in the 127–302 °C range in the thermogram (Fig. 2b). This evaluation was also supported by DSC analyses (Fig. 2c), in which lower temperature values of melting point and glass transition were observed in pristine CA ($T_g = 177$ °C, $T_m = 221$ °C) if compared to recovered CA ($T_g = 197$ °C, $T_m = 227$ °C). In the presence of these additives, a little difference in the decomposition temperature could also be identified in the temperature range between 338 and 438 °C with a maximum speed rate at 352 °C and 357 °C for pristine and recovered CA, respectively. The decomposition process produces approximately 60 % weight loss for both polymers, followed by another loss of 13–15 % due to the thermal decomposition of remaining products.

3.2. Synthesis of the composite cryogels

Several cryogels were synthesized to study the transition of the colloidal solution to gel. Different amounts of recycled CA were dispersed in acetone/water containing 5 mM NH_3 (60:40, v/v) to obtain solutions with different polymer concentrations (3, 4, 5 % w/v). The addition of ammonia to the dispersant solution was necessary to allow the polymer solution to gel (Fig. 3a). As a matter of fact, it was observed that no gelation occurred when CA was solubilized in acetone or acetone/water (60/40 v/v). The same results were obtained for all the studied polymer concentration levels (3, 4, 5 % w/v). The addition of ammonia plays a dual role: on the one hand, it facilitates the CA dispersion in acetone/water (60/40, v/v) promoting the partial deacetylation of the polymer; on the other hand, it favors the aggregation of polymer chains in a network incorporating the solvent. The removal of acetyl portions, and the consequent introduction of -OH groups, makes the polymer more polar: the creation of hydrogen bonds, favored by this new structure, allows the polymer chains to interact more strongly compared to the weak van der Waals interactions. These new interactions explain both the improved dispersion in a polar solvent system acetone/water (de Freitas et al., 2017) and gelation of CA (Howard and Parikh, 1968), not observed without the addition of ammonia.

3.2.1. Bulk density, porosity, and mechanical properties of the cryogels

The gravimetric method, thanks to the regular cylindrical shape of the cryogels (Fig. S5 shows the real dimensions of the 3D membranes), was used to calculate the material density. The observed trend (Fig. 4a) suggests how, increasing the polymer concentration, it is possible to obtain denser materials with a higher mechanical resistance, as confirmed by the Young's modulus of cryogels calculated from the stress-strain curve obtained in the compression experiment (see Fig. 4b) and by the results of ATR-FTIR analyses (see Section 3.2.2). In all cases, the synthesized materials were light with a density in the range 50–90 mg/cm^3.

The density values were used to calculate the total porosity of the material considering the formula reported in Section 2.7. The total porosity is concentration-dependent (Fig. 4c): as the concentration of the polymer solution increases, the porosity of the cryogel decreases. The same trend is observed for the interconnected porosity but, despite the high total porosity, relatively low values between 20 and 25 % were obtained (Fig. 4d). The porosity was also observed with SEM images using magnitudes of 100-500× on CA@AC-15 % (Fig. S6).

These results are in agreement with the studies by Buchtová et al. (2019) on cellulose gels. In their work, the authors highlight how the properties of the material can be modified by changing the concentration of the polymer solution. In particular, they observe that an increase in polymer solution concentration produces a reduction of the total porosity of aerogels and cryogels but, at the same time, a reduction in pore size and an increase in the surface area. They conclude that the increase in cellulose concentration leads to a division of pores into smaller ones, keeping pore wall thickness unchanged.

High mechanical resistance, good morphological properties in terms of high total porosity and surface area, and small pore size are desirable characteristics in sorbent materials to ensure stability during all operations and better contact with analytes. Considering what has just been said, the 5 % w/v cryogel was selected as the ideal polymer concentration to continue the studies.

3.2.2. ATR-FTIR spectroscopy of the cryogels

The comparison between the spectra of recovered CA and synthesized cryogels are reported in Fig. 5a. A sensible reduction in the absorption bands was observed in the range 1750–1730 cm^{-1} attributable to the C═O stretching of the ester bond and 1210–1163 cm^{-1} due to the C—O stretching of the ester bond. At the same time, absorption bands of -OH groups increase their signals between 3500 and 3000 cm^{-1} and 1420–1330 cm^{-1} due to the O—H stretching and bending of the polymer and adsorbed water, respectively; finally, an increase in the range 1120–1090 cm^{-1} is due to the C—O stretching of the secondary alcohols, obtained after the deacetylation. The results also support that gelation is mediated by strong hydrogen bonds between polymer chains.

3.2.3. Thermal gravimetric analysis (TGA) of the cryogels

The TGA curves in the range 25–430 °C of the cryogels and recovered CA are shown in Fig. 5b. For the recovered CA, a 3–4 % weight loss is observed between 27 and 127 °C, related to the sample dehydration. A major loss of hydration water (10 % of the total weight) is observed

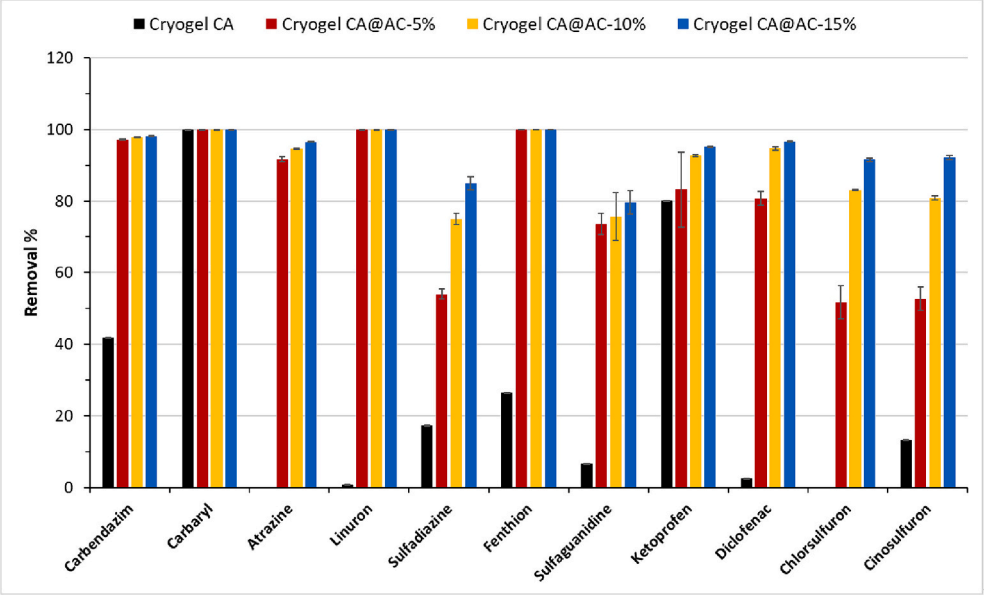

Fig. 6. Removal comparison of the different cryogels: without activated carbon (cryogelCA) and loaded with different amounts of activated carbon (CA@AC-5 %, CA@AC-10 %, CA@AC-15 %).

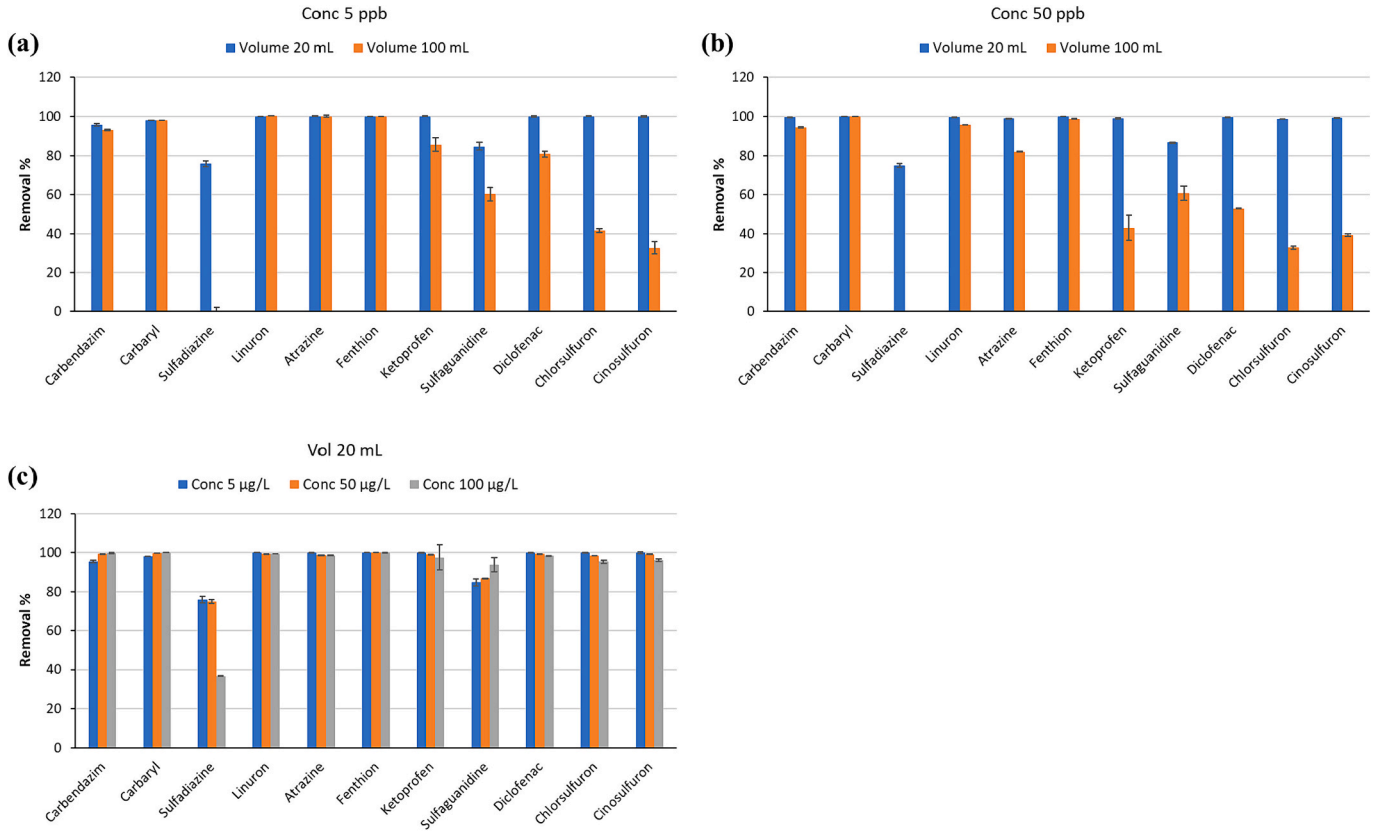

Fig. 7. Effect of treated volume on the removal % at 5 µg/L **(a)** and 50 µg/L **(b)**. **(c)** Effect of the analyte concentration on the removal % treating 20 mL of polluted water.

between 27 and 152 °C in the thermogram of cryogel, also after lyophilization, due to the higher polarity of the polymer that strongly retains water molecules in the network. The thermal decomposition of recovered CA occurs between 227 and 402 °C with a maximum speed rate around 352 °C, while it is observed in the range 277–377 °C for CA@AC-15 % w/v with maximum speed rate around 342 °C. Moreover, the slope reduction in the range of 277–377 °C suggests how the addition of AC could enhance the thermal stability of the material.

3.3. Adsorption study

Eleven organic contaminants, often detected in river water, were

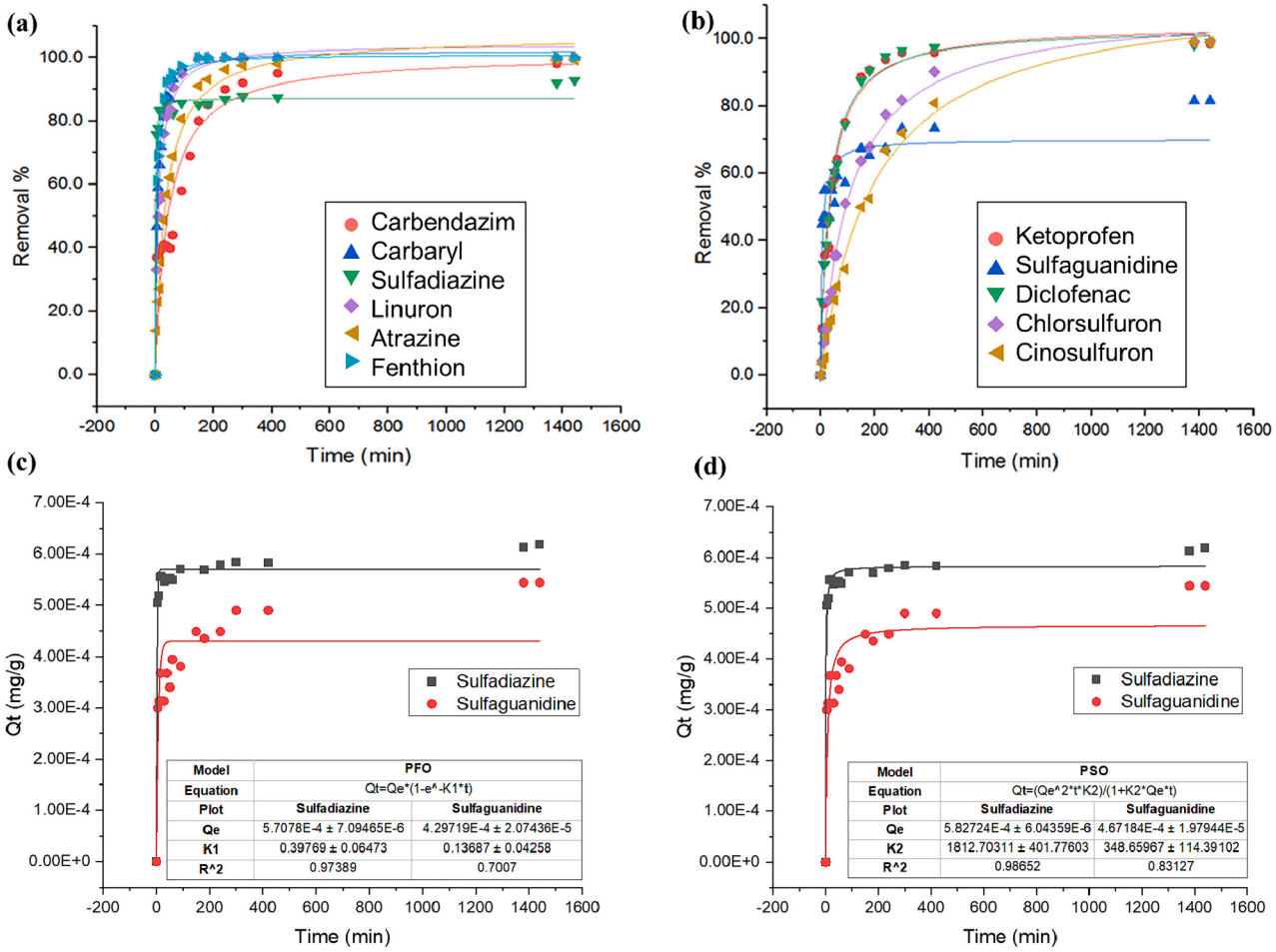

Fig. 8. **(a)** and (**b**) Kinetic study in 20 mL of spiked river water at 5 μg/L in 24 h. (**c**) and (**d**) Pseudo-first order (PFO) and pseudo-second order (PSO) kinetics model, applied to the most polar analytes studied (sulfadiazine and sulfaguanidine), for which the removal was high but not total. Experimental condition: 20 mL of spiked river water at 5 μg/L from 0 to 24 h.

selected as model compounds on the basis of their different structures, logP and pKa values, and their uses (Table S2).

A river water sample (20 mL spiked at 5 μg/L) was used to evaluate the analytical performance of the 3D membranes. Table S3 lists the main figures of merit of the analysis method (Section 2.1), while Fig. 6 and Table S4 display the effect of the AC amounts, loaded into the cryogels, on the removal percentage. The results show how small amounts of AC greatly increase the removal yields of the organic contaminants, compared to the cryogel CA. In particular, an average removal of 90.6 % can be reached when an AC load of 15 % w/w is used (Table S4). The lowest removal yield (79 %) is achieved for sulfaguanidine, the most polar analyte, probably due to worse retention on the composite cryogel. Moreover, after 24 h the remaining concentration for carbendazim, carbaryl, linuron, and fenthion was lower than the LOD and LOQ of the method (Table S3). It is worth underling that, when the CA cryogel was used to treat the water, carbaryl and ketoprofen were efficiently removed (100 % and 80 %, respectively) with a residual concentration lower than their LODs in the treated water sample.

The effects of the treated water volume and analyte concentration were studied over 24 h by selecting the cryogel CA@AC-15 %. As shown in Fig. 7a and b, scaling down the sample volume from 100 to 20 mL, and using two different spike levels (5 and 50 μg/L), better results were always obtained with the lowest volume being the analyte diffusion the limiting step. However, the study of the concentration effect in the range of 5–100 μg/L (Fig. 7c) indicates how highly polluted water can be treated without losing performance, even if, processing higher volumes, lesser percentages of removal are achieved especially for very polar compounds (sulfadiazine), probably due to a competitive adsorption process by the nonpolar substances.

The kinetic study was also performed to better understand the time required to reach the equilibrium (Fig. 8). The faster kinetics (<400 min) were observed for fenthion, sulfadiazine, linuron, ketoprofen, and diclofenac (Fig. 8a and b), while lower trends for atrazine, carbendazim, chlorsulfuron, cinosulfuron, and sulfaguanidine (>400 min). Considering the challenge of removing highly polar organic contaminants from water, pseudo-first order and pseudo-second order kinetic models were applied to investigate the behavior of the CA@AC-15 % toward sulfonamide compounds (sulfaguanidine and sulfadiazine), the least removed from water during the experiment (Fig. 8c and d).

Fig. 8c and d show the plot and the parameters q_e, k_1, k_2 and R^2 for the two analytes. The experimental data, obtained in competitive adsorption conditions, prove that the pseudo-second order model exhibits the best fit with R^2 of 0.9865 and 0.8313 for sulfadiazine and sulfaguanidine, respectively. These results suggest that the slow step of the sorption process is the adsorption into the multiple active sites of the composite cryogel (Wang and Guo, 2020).

The observed trends clearly suggest how the chemical structures and hydrophobicity of contaminants influence the rate of adsorption onto the activated sites of the sorbent. In particular, the graphitic structure of AC it is expected to provide strong π-π interactions with the aromatic moieties of the analytes compared to the bare structure of CA, while hydrogen bonds and van der Waals interactions ensure the adsorption of the more polar compounds.

4. Conclusion

In the present work, a simple and fast protocol to recover CA from CBs is presented. The regenerated CA shows thermal and spectroscopical properties comparable to pristine CA from unused CFs. The recovered polymer was used to synthesize, through a sol-gel phase transition process, porous and robust cryogels using AC as filler to increase the adsorption capability of the 3D membranes. The devices were tested to adsorb eleven selected organic contaminants, commonly found in river water. In adsorption tests, the cryogel containing 15 % w/w of AC showed high efficiency in the treatment (>79 %) of heavily polluted waters (5–100 μg/L), even if the results and removal values indicated that diffusion was limiting for 6 out of 11 analytes when larger volumes of water were treated (100 mL). These results bode well for a possible recycling of CA on a pilot scale and its application in water treatment rescaling the device to make it more performant in the treatment of higher water volumes. The device is also promising on analytical scale as a sustainable sorbent to perform solid phase extractions mediated by membranes (Bosco et al., 2023) using carbon nanomaterials as fillers.

CRediT authorship contribution statement

Massimo Giuseppe De Cesaris: Validation, Methodology, Data curation, Conceptualization. **Nina Felli:** Writing – original draft, Formal analysis. **Lorenzo Antonelli:** Software, Formal analysis. **Iolanda Francolini:** Methodology, Investigation, Conceptualization. **Giovanni D'Orazio:** Investigation, Conceptualization. **Chiara Dal Bosco:** Software, Formal analysis. **Alessandra Gentili:** Writing – review & editing, Visualization, Supervision, Project administration.

Declaration of competing interest

The authors declare that they have no known competing financial interests or personal relationships that could have appeared to influence the work reported in this paper.

Data availability

No data was used for the research described in the article.

Acknowledgments

This work was supported by Sapienza University of Rome, Research start-up projects for young researchers - Type 1. Protocol number: 1AR1221816C7498C6.

Appendix A. Supplementary data

Supplementary data to this article can be found online at https://doi.org/10.1016/j.scitotenv.2024.172677.

References

Abu-Danso, E., Bagheri, A., Bhatnagar, A., 2019. Facile functionalization of cellulose from discarded cigarette butts for the removal of diclofenac from water. Carbohydr. Polym. 219, 46–55. https://doi.org/10.1016/j.carbpol.2019.04.090.

Antonelli, L., Frondaroli, M.C., De Cesaris, M.G., Felli, N., Dal Bosco, C., Lucci, E., Gentili, A., 2024. Nanocomposite microbeads made of recycled polylactic acid for the magnetic solid phase extraction of xenobiotics from human urine. Microchim. Acta 191 (5), 1–14. https://doi.org/10.1007/s00604-024-06335-y.

Bialous, S., Curtin, C., Tursan d'Espaignet, E., 2017. Tobacco and its Environmental Impact: An Overview. World Health Organization, Geneva, Switzerland. ISBN 978-92-4-151249-7.

Bonanomi, G., Incerti, G., Cesarano, G., Gaglione, S.A., Lanzotti, V., 2015. Cigarette butt decomposition and associated chemical changes assessed by 13C CPMAS NMR. PLoS One 10 (1). https://doi.org/10.1371/journal.pone.0117393.

Bosco, C.D., De Cesaris, M.G., Felli, N., Lucci, E., Fanali, S., Gentili, A., 2023. Carbon nanomaterial-based membranes in solid-phase extraction. Microchim. Acta 190 (5), 175. https://doi.org/10.1007/s00604-023-05741-y.

Buchtová, N., Pradille, C., Bouvard, J.L., Budtova, T., 2019. Mechanical properties of cellulose aerogels and cryogels. Soft Matter 15 (39), 7901–7908. https://doi.org/10.1039/C9SM01028A.

Conradi, M., Sánchez-Moyano, J.E., 2022. Toward a sustainable circular economy for cigarette butts, the most common waste worldwide on the coast. Sci. Total Environ. 847, 157634 https://doi.org/10.1016/j.scitotenv.2022.157634.

D'Ascenzo, G., Gentili, A., Marchese, S., Perret, D., 1998. Development of a method based on liquid chromatography–electrospray mass spectrometry for analyzing imidazolinone herbicides in environmental water at part-per-trillion levels. J. Chromatogr. A 800 (1), 109–119. https://doi.org/10.1016/S0021-9673(97)00860-1.

De Fenzo, A., Giordano, M., Sansone, L., 2020. A clean process for obtaining high-quality cellulose acetate from cigarette butts. Materials 13 (21), 4710. https://doi.org/10.3390/ma13214710.

de Freitas, R.R., Senna, A.M., Botaro, V.R., 2017. Influence of degree of substitution on thermal dynamic mechanical and physicochemical properties of cellulose acetate. Ind. Crop. Prod. 109, 452–458. https://doi.org/10.1016/j.indcrop.2017.08.062.

DIRECTIVE (EU) 2019/904 OF THE EUROPEAN PARLIAMENT AND OF THE COUNCIL of 5 June 2019 on the reduction of the impact of certain plastic products on the environment, Official Journal of the European Union L 155/1-19.

ErionCare. https://erioncare.it/it/. (Accessed 19 April 2024).

Fahanwi, A.N., Yasir, M., Nguyen, H.T., Saha, N., Saha, T., Sedlařík, V., Saha, P., 2024. In situ polyaniline polymerization on electrospun cellulose acetate nanofibers derived from recycled waste filter butts of cigarettes for the enhanced removal of methyl orange and rhodamine. Chem. Eng. Res. Des. 201, 18–30. https://doi.org/10.1016/j.cherd.2023.11.043.

Green, D.S., Tongue, A.D., Boots, B., 2022. The ecological impacts of discarded cigarette butts. Trends Ecol. Evol. 37 (2), 183–192. https://doi.org/10.1016/j.tree.2021.10.001.

Hamzah, Y., Umar, L., 2017, May. Preparation of creating active carbon from cigarette filter waste using microwave-induced KOH activation. In: Journal of Physics: Conference Series, Vol. 853, No. 1. IOP Publishing, p. 012027. https://doi.org/10.1088/1742-6596/853/1/012027.

Howard, P., Parikh, R.S., 1968. Solution properties of cellulose triacetate. II. Solubility and viscosity studies. J. Polym. Sci., Part A-1: Polym. Chem. 6 (3), 537–546. https://doi.org/10.1002/pol.1968.150060310.

Hummel, A., 2004, March. 3.2 industrial processes. In: Macromolecular Symposia, Vol. 208, No. 1. WILEY-VCH Verlag, Weinheim, pp. 61–80. https://doi.org/10.1002/masy.200450406.

Kosior, E., Crescenzi, I., 2020. Solutions to the plastic waste problem on land and in the oceans. In: Plastic Waste and Recycling. Academic Press, pp. 415–446. https://doi.org/10.1016/B978-0-12-817880-5.00016-5.

LEGGE 28 dicembre 2015, n. 221 Disposizioni in materia ambientale per promuovere misure di green economy e per il contenimento dell'uso eccessivo di risorse naturali. (16G00006) (GU Serie Generale n.13 del 18-01-2016).

Lima, H.H., Maniezzo, R.S., Kupfer, V.L., Guilherme, M.R., Moises, M.P., Arroyo, P.A., Rinaldi, A.W., 2018. Hydrochars based on cigarette butts as a recycled material for the adsorption of pollutants. J. Environ. Chem. Eng. 6 (6), 7054–7061. https://doi.org/10.1016/j.jece.2018.11.012.

Mahto, A., Halakarni, M.A., Maraddi, A., D'Souza, G., Samage, A.A., Thummar, U.G., Nataraj, S.K., 2022. Upcycling cellulose acetate from discarded cigarette butts: conversion of contaminated microfibers into loose-nanofiltration membranes for selective separation. Desalination 535, 115807. https://doi.org/10.1016/j.desal.2022.115807.

Marinello, S., Lolli, F., Gamberini, R., Rimini, B., 2020. A second life for cigarette butts? A review of recycling solutions. J. Hazard. Mater. 384, 121245 https://doi.org/10.1016/j.jhazmat.2019.121245.

Moroz, I., Scapolio, L.G., Cesarino, I., Leão, A.L., Bonanomi, G., 2021. Toxicity of cigarette butts and possible recycling solutions—a literature review. Environ. Sci. Pollut. Res. 28, 10450–10473. https://doi.org/10.1007/s11356-020-11856-z.

Nabwey, H.A., Abdelkreem, M., Tony, M.A., Al Hoseny, N.F., 2024. Smart win–win waste management: superhydrophobic filter using valorized cellulose acetate from discarded cigarette butts for cleaning up marine oil spill at Hurghada Red Sea shore in Egypt. Front. Mar. Sci. 11, 1270026 https://doi.org/10.3389/fmars.2024.1270026.

Novotny, T.E., Slaughter, E., 2014. Tobacco product waste: an environmental approach to reduce tobacco consumption. Curr. Environ. Health Rep. 1, 208–216. https://doi.org/10.1007/s40572-014-0016-x.

Puls, J., Wilson, S.A., Hölter, D., 2011. Degradation of cellulose acetate-based materials: a review. J. Polym. Environ. 19, 152–165. https://doi.org/10.1007/s10924-010-0258-0.

Shah, G., Bhatt, U., Soni, V., 2023. Cigarette: an unsung anthropogenic evil in the environment. Environ. Sci. Pollut. Res. 1-12 https://doi.org/10.1007/s11356-023-26867-9.

Soleimani, F., Dobaradaran, S., De-la-Torre, G.E., Schmidt, T.C., Saeedi, R., 2022. Content of toxic components of cigarette, cigarette smoke vs cigarette butts: a comprehensive systematic review. Sci. Total Environ. 813, 152667 https://doi.org/10.1016/j.scitotenv.2021.152667.

Torkashvand, J., Farzadkia, M., 2019. A systematic review on cigarette butt management as a hazardous waste and prevalent litter: control and recycling. Environ. Sci. Pollut. Res. 26, 11618–11630. https://doi.org/10.1007/s11356-019-04250-x.

Torkashvand, J., Saeedi-Jurkuyeh, A., Rezaei Kalantary, R., Gholami, M., Esrafili, A., Yousefi, M., Farzadkia, M., 2022. Preparation of a cellulose acetate membrane using cigarette butt recycling and investigation of its efficiency in removing heavy metals from aqueous solution. Sci. Rep. 12 (1), 20336. |. https://doi.org/10.1038/s41598-022-24432-x.

Vasseghian, Y., Alimohamadi, M., Dragoi, E.N., Sonne, C., 2023. A global meta-analysis of phthalate esters in drinking water sources and associated health risks. Sci. Total Environ., 166846 https://doi.org/10.1016/j.scitotenv.2023.166846.

Wang, J., Guo, X., 2020. Adsorption isotherm models: classification, physical meaning, application and solving method. Chemosphere 258, 127279. https://doi.org/10.1016/j.chemosphere.2020.127279.

Wang, M., You, X.Y., 2021. Critical review of magnetic polysaccharide-based adsorbents for water treatment: synthesis, application and regeneration. J. Clean. Prod. 323, 129118 https://doi.org/10.1016/j.jclepro.2021.129118.

Wienk, I.M., Folkers, B., van den Boomgaard, T., Smolders, C.A., 1994. Critical factors in the determination of the pore size distribution of ultrafiltration membrances using the liquid displacement method. Sep. Sci. Technol. 29 (11), 1433–1440. https://doi.org/10.1080/01496399408003029.